

Remote Sensing of Surface Ocean Circulation with Satellite Altimetry

R. S. Mather, C. Rizos, R. Coleman

The gravitationally stabilized Geodynamics Experimental Ocean Satellite (GEOS-3) spacecraft (Fig. 1A) was launched in April 1975 with an orbital period of 101.79 minutes and an inclination of 115°. In addition to the usual instrumentation for accurate position fixing, it also carries a 13.9-gigahertz radar altimeter for measuring the vertical distance to the sea surface. Included in the design requirements for the altimeter in the short-pulse mode was a precision of ± 50 centimeters from averages over 0.1 second such that the correlation of random error in the averaging procedure was held to below .33 (1). As the spacecraft is moving at approximately 7 kilometers per second, each data point has a finite footprint. If one is considering the local sea state, the analysis of 1-second averages imposes a 15-km limit on the shortest wavelength of information recoverable from GEOS-3 altimeter data of this type (2).

Figure 1B illustrates the relationship between the altimeter range h , the height N of the geoid (datum level surface), the height ζ of the stationary sea surface above the reference ellipsoid, and the dynamic sea-surface topography (SST) ζ_s . The last three quantities are related by

$$\zeta_s = \zeta - N \quad (1)$$

The horizontal gradients of ζ_s are one of the factors influencing the circulation of the surface layer of the ocean through the equations (3)

$$\ddot{x}_1 - f\dot{x}_2 = -g \frac{d\zeta_s}{dx_1} - \frac{1}{\rho_w} \frac{dp_a}{dx_1} + F_1 \quad (2a)$$

$$\ddot{x}_2 + f\dot{x}_1 = -g \frac{d\zeta_s}{dx_2} - \frac{1}{\rho_w} \frac{dp_a}{dx_2} + F_2 \quad (2b)$$

The velocities of the known steady-state ocean currents never exceed 300 cm/sec (4). It follows from Eq. 2 that gradients of ζ_s cannot exceed 3 meters per 10^2 km at mid-latitudes.

Furthermore, as the steady-state wind velocities seldom exceed 50 m/sec, the resulting velocities of the ocean surface layer are less than 50 cm/sec (3). The changes produced in gradients of ζ_s at

Summary. The Geodynamics Experimental Ocean Satellite (GEOS-3) radar altimeter has provided some information on the dynamic sea-surface topography of the global oceans. Regional studies of the densely surveyed Sargasso Sea indicate that the average nontidal variability of the oceans is ± 28 centimeters. Sea-surface highs and lows determined from GEOS-3 altimetry correlate favorably with eddy structures inferred from Nimbus-6 infrared imagery.

mid-latitudes are less than 50 cm/ 10^2 km. The errors in GEOS-3 altimeter data must be below ± 20 cm/ 10^2 km if these data are to be used in mapping steady-state currents. An improvement of a factor of 5 is needed if such data are to be used in determining the changes of ζ_s with time that are associated with variations in the surface circulation.

At first glance, it would appear that the signal-to-noise problems preclude the recovery of information related to ocean circulation from GEOS-3 altimeter data. The principal difficulties are the following:

1) The data were collected only between parallels 65°N and 65°S (Fig. 2A). This, together with the absence of recording facilities on-board GEOS-3, limits the available surface coverage, for a 5-day sample, to that shown in Fig. 2B.

2) The altimetry measurements were recorded in the form of discrete passes

never exceeding 9000 km in length. The data were, for the most part, collected on a regional rather than a global basis, the acquisition areas and periods being governed by the location of transportable telemetry units. These instruments occupied any given site for periods up to 3 months.

3) The precision of the orbit determination was variable. The analysis of orbits based on Doppler tracking data indicated a root-mean-square (rms) radial error of ± 1.3 m (5). This figure reduces to ± 0.9 m in the case of a GEOS-3 ephemeris based on laser tracking data supplemented with S-band tracking only where needed (6). The major source of error is probably the model of the earth's gravity field used in orbit integration. The best models available at present are the Goddard earth model (GEM) series. The latest set consists of GEM 9, based on satellite data only, and GEM 10, obtained from a combination of satellite and surface data (7).

4) The datum level surface (geoid) needs to be defined in ocean areas with a precision of better than ± 20 cm/ 10^2 km through shorter wavelengths. It has been conventional to assume that such determinations are obtained from surface gravity and elevation data which are related to the geoid (8). The desired precision cannot be obtained directly because (i) the gravity data in ocean areas are not of sufficient quality or density to allow reliable computations of a gravimetric geoid; and (ii) the relevant data in the form of gravity anomalies, if assumed to be of adequate quality, nevertheless are

When this article was written, Dr. Mather was a senior resident research associate of the U.S. National Research Council at Goddard Space Flight Center, Greenbelt, Maryland 20771. Drs. Rizos and Coleman were research associates at the Department of Earth and Planetary Sciences, Johns Hopkins University, Baltimore, Maryland 21218. All three authors were on leave from the Department of Geodesy, University of New South Wales, Sydney, Australia. Dr. Mather died on 7 September 1978.

related to the sea surface and not the geoid.

Despite these adverse factors, it is possible to obtain some information on the following parts of the spectrum of dynamic SST in both space and time from GEOS-3 altimetry.

Quasi-stationary components of very long wavelength for which gravity field components are known to better than 1 part in 10^8 . These are zonal harmonic terms, principally of degree 2 (ζ_{s120}), and to a lesser extent of degrees 3 (ζ_{s130}) and 4 (ζ_{s140}), in the global surface spherical harmonic expansion of ζ_s given by

$$\zeta_s = \sum_{n=1}^{\infty} \sum_{m=0}^n \sum_{\alpha=1}^2 \zeta_{s\alpha nm} S_{\alpha nm} \quad (3)$$

where $\zeta_{s\alpha nm}$ are coefficients of degree n and order m , $S_{\alpha nm}$ being surface spherical harmonic functions defined by

$$S_{1nm} = P_{nm}(\sin \phi) \cos m\lambda \quad (4a)$$

$$S_{2nm} = P_{nm}(\sin \phi) \sin m\lambda \quad (4b)$$

where $P_{nm}(\sin \phi)$ are normalized associated Legendre functions (9).

Time-varying components of ζ_s with wavelengths between 50 and 500 km and amplitudes in excess of 30 cm. Oceanographic phenomena of interest in this part of the spectrum are ocean eddies which have been extensively studied in recent years. Eddies have long been observed near the strong western boundary currents, such as the Gulf Stream (10). Although the formation of eddies has been well documented, there is still much to be learned about their movements and life histories.

A study of the power spectrum of the stationary dynamic SST (the signal), as estimated by oceanographers (11), in re-

lation to that of the estimated errors in the GEM 9 gravity field model (the noise) shows that it is not possible to recover any harmonics in ζ_s of degree greater than or equal to 4 (12) (except perhaps the zonal coefficient ζ_{s160}). This follows because the degree variance of the SST ($V\zeta$), given by

$$V\zeta_n = \sum_{m=0}^n \sum_{\alpha=1}^2 \zeta_{s\alpha nm}^2 \quad (5)$$

for degree n , is less than the degree variance of the error in GEM 9 for $n > 4$. The coefficients $\zeta_{s\alpha nm}$ in Eq. 3 used to estimate the expected variance in Eq. 5 are obtained by the analysis of steric anomalies computed from surface measurements of temperature and salinity to depths of 2000 m (11). To facilitate the direct comparison with results from the GEOS-3 data, the ocean area is defined as those regions that were scanned by the altimeter. The numerical values of $\zeta_{s\alpha nm}$ change if this definition is altered (13). A more specific examination of the individual coefficients obtained in this manner shows that the signal-to-noise ratio is favorable for the recovery of the six dominant coefficients in the global representation of ζ_s . In decreasing order of magnitude, these dominant coefficients are ζ_{s100} , ζ_{s120} , ζ_{s111} , ζ_{s140} , ζ_{s110} , and ζ_{s130} .

The GEOS-3 Altimeter Data Bank

The data are in the form of discrete passes of lengths up to 9000 km. An orbital ephemeris was prepared under the supervision of the National Aeronautics and Space Administration (NASA) Wallops Flight Center (WFC) (called Wal-

lops orbits in this article). These orbits are based primarily on Doppler tracking data. The ephemeris used in this study was computed at either the NASA Goddard Space Flight Center (GSFC) or the U.S. Naval Surface Weapons Center (NSWC), using dynamic satellite reduction techniques. A smaller set of orbits was based primarily on high-precision laser tracking data (6). The times of the altimeter ranges are correlated with the GEOS-3 ephemeris to define ζ (Eq. 1). The accuracy with which this correlation is performed is critical as the rate of change of the altimeter range can be as large as 20 m/sec. For example, a time tagging correlation error of 1 millisecond can cause an error in ζ of 2 cm.

The difference between values of ζ obtained by this method and the gravimetrically determined N values (Eq. 1) should not exceed ± 2 m. Nevertheless, the data originally provided to investigators by WFC showed differences due to time tag errors that were sometimes in excess of ± 10 m. As the true variation of ζ over short periods of time is unlikely to exceed ± 60 cm, the analysis of cross-overs of GEOS-3 ground tracks (Fig. 2B) during some limited time span leads to the following conclusions (14). (i) The crossover discrepancies in ζ based on Wallops orbits, after the exclusion of approximately 12 percent of the passes, indicated that the radial component of orbital error was in the range ± 1.3 m. In the case of laser orbits (6), the figure was ± 0.9 m. These Wallops orbits are suitable for global studies. (ii) The rms error can be reduced to ± 0.3 m for regional studies covering up to 4×10^6 km² if individual passes are treated as internally consistent but subject to unknown "or-

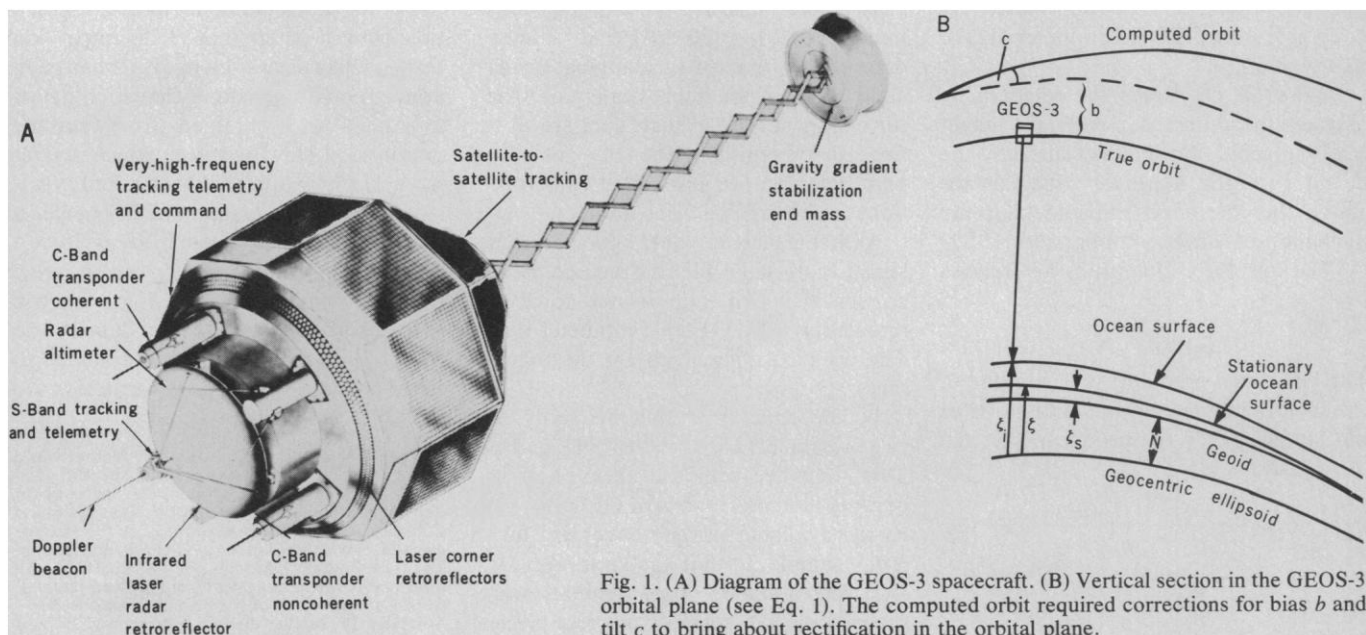


Fig. 1. (A) Diagram of the GEOS-3 spacecraft. (B) Vertical section in the GEOS-3 orbital plane (see Eq. 1). The computed orbit required corrections for bias b and tilt c to bring about rectification in the orbital plane.

bital'' errors which can be modeled by a constant bias (b) and a tilt (c) (Fig. 1B).

The application of b and c corrections per pass also eliminates portions of the spectrum of ζ_s . However, the resulting data are less noisy and therefore suitable for differential regional studies of ζ_s and its variations with time. Although global solutions are subject to higher noise levels, they retain all information on ζ_s with wavelengths greater than 10^3 km. Regional solutions over an area d^2 (in square kilometers) do not contain information on ζ_s with wavelengths greater than $2d$ because of the application of b and c corrections. However, the noise is smaller by a factor of 4.

Parameters of the Quasi-Stationary Component

Only the six harmonic coefficients listed earlier can be recovered from the best gravity field model available at the present time, if the satellite altimetry is free of error. However, the altimetry data are not free of error. Any solution procedure would fail if errors in the altimetry data had the same wavelengths as those sought in the SST.

The term of zero degree ($\zeta_{s100} = 1.15$

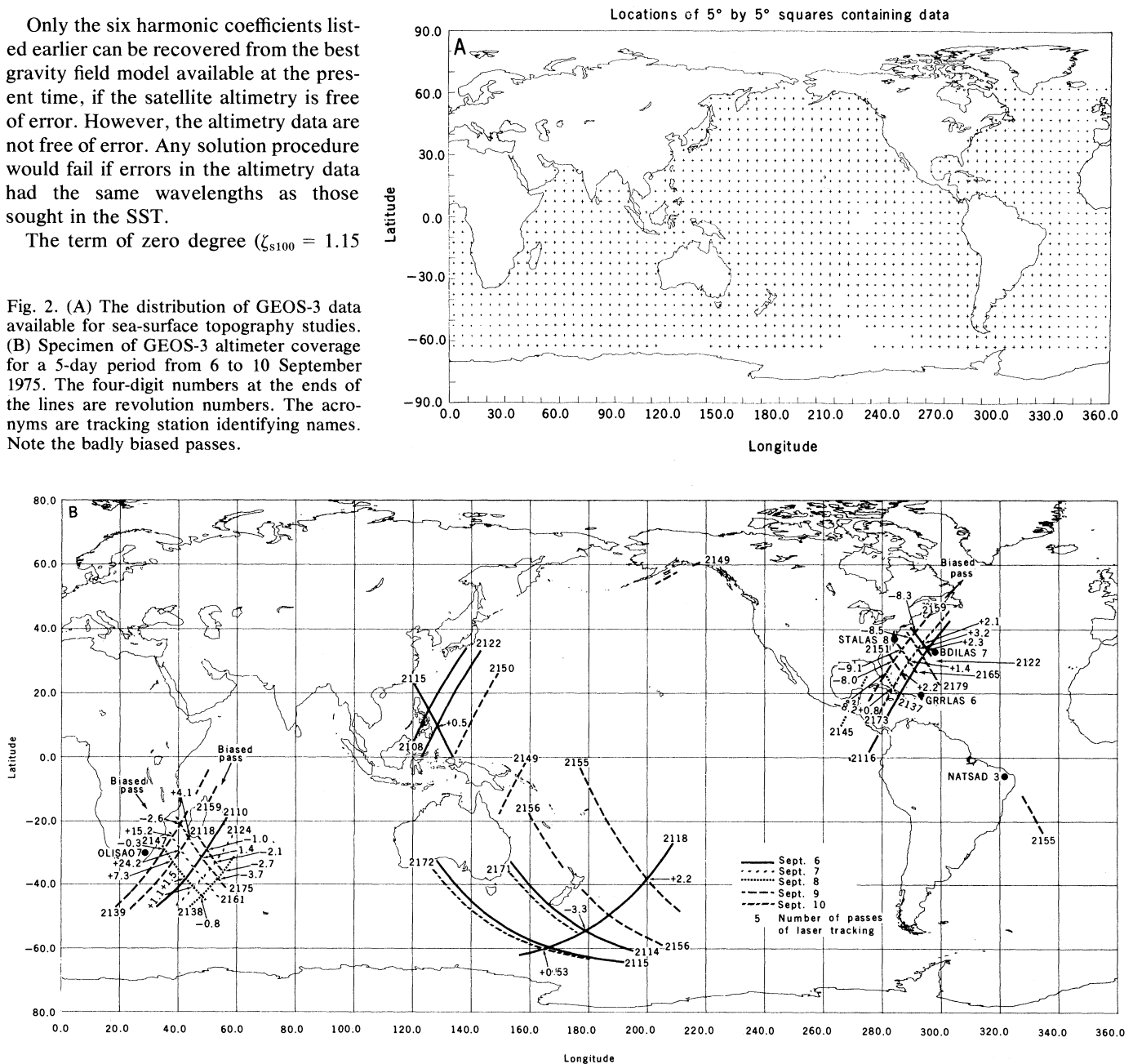
m) obtained from the global analysis of steric anomalies is not of relevance as it is incorporated in the definition of the geoid. The dominant term is therefore the second-degree zonal harmonic ($\zeta_{s120} = -46$ cm) (Table 1). The GEOS-3 altimetry as acquired during any 5-day period traces a partial global grid of ground tracks (Fig. 2B). The quality of the tracking is reflected in the average crossover discrepancy. A second means of assessing the quality of ζ values generated from the altimetry is to study the variation of values of ζ within a 1° by 1° square. The value of N varies with position within such a square with an rms error of ± 0.3 to ± 0.8 m. The variation of ζ_s within such a region does not materially alter these figures for changes in ζ over the same area. The values obtained are a

function of the orbits, varying from ± 1.7 to ± 2.1 m for Wallops orbits and reducing to ± 1.3 m for laser orbits (Table 1). These figures tend to confirm the estimates obtained from the cross-over analysis for the radial component of the orbital error.

Global solutions are noisy but have the advantage of being related to the orbits. The latter are referred to a geocentric reference system with origin at the geocenter (earth's center of mass) and oriented in relation to the conventional international origin (CIO) and the meridian of zero longitude as defined by the Bureau International de l'Heure (15).

These solutions require a set of stationary ζ values in the form of 1° by 1° equiangular means prepared with the use of the best available orbits so that no in-

Fig. 2. (A) The distribution of GEOS-3 data available for sea-surface topography studies. (B) Specimen of GEOS-3 altimeter coverage for a 5-day period from 6 to 10 September 1975. The four-digit numbers at the ends of the lines are revolution numbers. The acronyms are tracking station identifying names. Note the badly biased passes.



formation on low-degree contributions to the shape of the sea surface is lost. The tidal signal has been largely eliminated in the process of averaging the data. The geoid model defined by GEM 9 was differenced from the grid of sea-surface heights. (These residual heights would in fact be the quasi-stationary component of the SST as a continuous field if the GEM 9 geoid were free from error for all wavelengths.) The residual heights, however, allowed a determination of the dominant harmonic coefficients, as they did not contain errors equivalent in wavelength and amplitude to the SST.

We have also obtained solutions based on the use of long passes of GEOS-3 altimetry after the noise levels have been reduced to ± 80 cm by the application of

b and c corrections. However, the adoption of such a procedure loses information with wavelengths greater than twice the length of the pass. The exception is information on harmonics that are symmetrical about the equator. Table 1 lists the coefficients obtained from various subsets of the GEOS-3 altimetry data bank at GSFC derived from both Wallops and laser orbits.

The solutions reported are the following:

1) The equinox data set contains over 310,000 records of GEOS-3 altimeter data collected between 25 August and 5 November 1975 and between 25 February and 5 May 1976. Under ideal circumstances, parameters of the global SST computed from this data set would be

minimally affected by seasonal variations. This data set provides a 49.3 percent coverage of the oceans within the parallels 65°S and 65°N, excluding inland seas. Both Wallops and laser orbits were used to obtain solutions from this data set.

2) The Wallops 1976 data set, based on over 350,000 data points collected during the first 8 months of 1976, was examined because it had the smallest cross-over discrepancies based on the use of Wallops orbits. This does not necessarily mean that the orbits for other periods were inferior as there may be some time tag problems associated with the data.

3) The Wallops complete data set included 850,000 data points. Over half of these data, recorded during the earlier part of the period from April 1975 to August 1976, were subject to higher levels of noise. This data set provides a 80.1 percent coverage of the oceans.

4) The long-pass solution was the only data set prepared after the use of b and c corrections to reduce orbital noise. We computed these corrections for long passes by fitting the data, pass by pass, to the best available gravity field model and simultaneously solving for the shape of the sea surface.

The results in Table 1 highlight the inability to recover the comparatively large coefficients of first degree (ζ_{S111} , ζ_{S110}) at the present time due to the non-geocentricity of the system of reference used in integrating the GEOS-3 orbits. The values obtained for these coefficients can be expected to change with the system of reference used.

The three zonal harmonics of degrees 2, 3, and 4 as obtained from the different solutions are in good agreement with the values obtained from the analysis of steric anomalies. The rms variation per 1° by 1° square is probably a good indicator of the quality of the solution in each case (Table 1). The unweighted mean value obtained for the normalized second-degree zonal coefficient ζ_{S120} is -42 ± 3 cm, which compares with -46 cm obtained from steric anomalies after allowing for the effect of the permanent earth tide (16) and incomplete sampling. Values obtained for the other dominant zonal coefficients are listed in Table 1.

As far as we know, truncated surface spherical harmonic series for modeling the global dynamic sea-surface topography have not been used by oceanographers. Figure 3 illustrates the representation obtained from a model to degree 16 (289 coefficients). The zonal harmonics of degrees 2, 3, and 4 obtained from GEOS-3 altimetry are supplemented by oceanographically determined values to

Table 1. Determinations of the dominant parameters of the stationary global sea-surface topography from various subsets of GEOS-3 altimetry in the global mode.

Normalized coefficient			Oceanographic* solution (cm)		Orbital solutions (cm)				Long-pass solutions (cm)
α	n	m	Global	Equinox representation	Wallops equinox	Laser equinox	Wallops, 1976	Wallops, complete	
1	1	0	+7	+10	-127†	-22†	-161†	-137†	
1	1	1	-22	-21	-1†	-72†	+7†	-5†	
1	2	0	-46	-44	-46‡	-54‡	-47‡	-47‡	-45‡
1	3	0	+7	+7	+14	+10	+13	+10	+2
1	4	0	-10	-10	-11	-10	-18	-12	-7
rms variation per 1° by 1° square					174	133	178	205	80
					Number of 1° blocks				
					16,707	16,575	14,782	27,171	
					Number of data points				
					310,920	308,401	367,762	875,273	27,674

*Between 65°S and 65°N from a spherical harmonic solution to degree 16 and order 16. †Includes the nongeocentricity of the reference coordinate system. ‡These values should be corrected by +6 cm for the permanent earth tide.

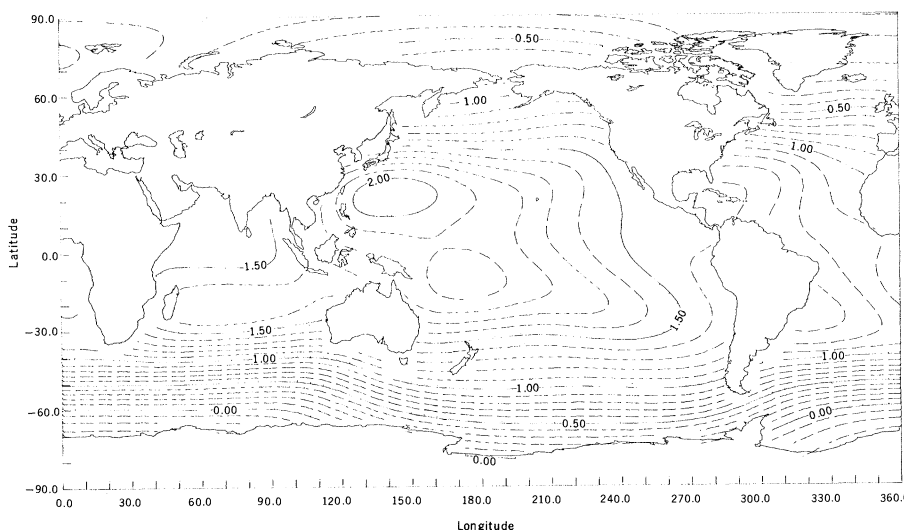


Fig. 3. A composite surface spherical harmonic representation of the dynamic sea-surface topography from GEOS-3 altimetry (zonal coefficients of degrees 2, 3, and 4) and steric anomalies (balance coefficients to degree 16). Contours are in meters with reference to an arbitrary datum.

the required degree. The lack of fit of the resulting model to the oceanographic data, due to the effect of truncation, is ± 9 cm. Models of this type can be easily converted to geostrophic components of the surface current vector if a non-accelerated system is assumed.

Time Variations in the Sargasso Sea

Since surface measurements give the eddy kinetic energy of the oceans as varying between 400 and 2000 cm^2/sec (17), the expected variations in ζ_s due to eddy formation and decay can be as large as 10^2 cm with half wavelengths of 10^2 km (18, 19). The minimum useful resolution of variations of ζ_s with time from GEOS-3 altimeter data is ± 50 cm. Global solutions cannot meet this goal at the present time. GEOS-3 ground tracks almost repeat themselves every 526 revolutions. The comparison of pairs of such overlapping passes shows that the rms discrepancy between any pair can, with some minimal editing, be reduced to around ± 30 cm if the Nyquist limit (20) is taken to be 15 km (21). This figure can be 50 percent higher in the vicinity of fast-flowing currents. These results are obtained after each pass is subject to b and c corrections (Fig. 1B).

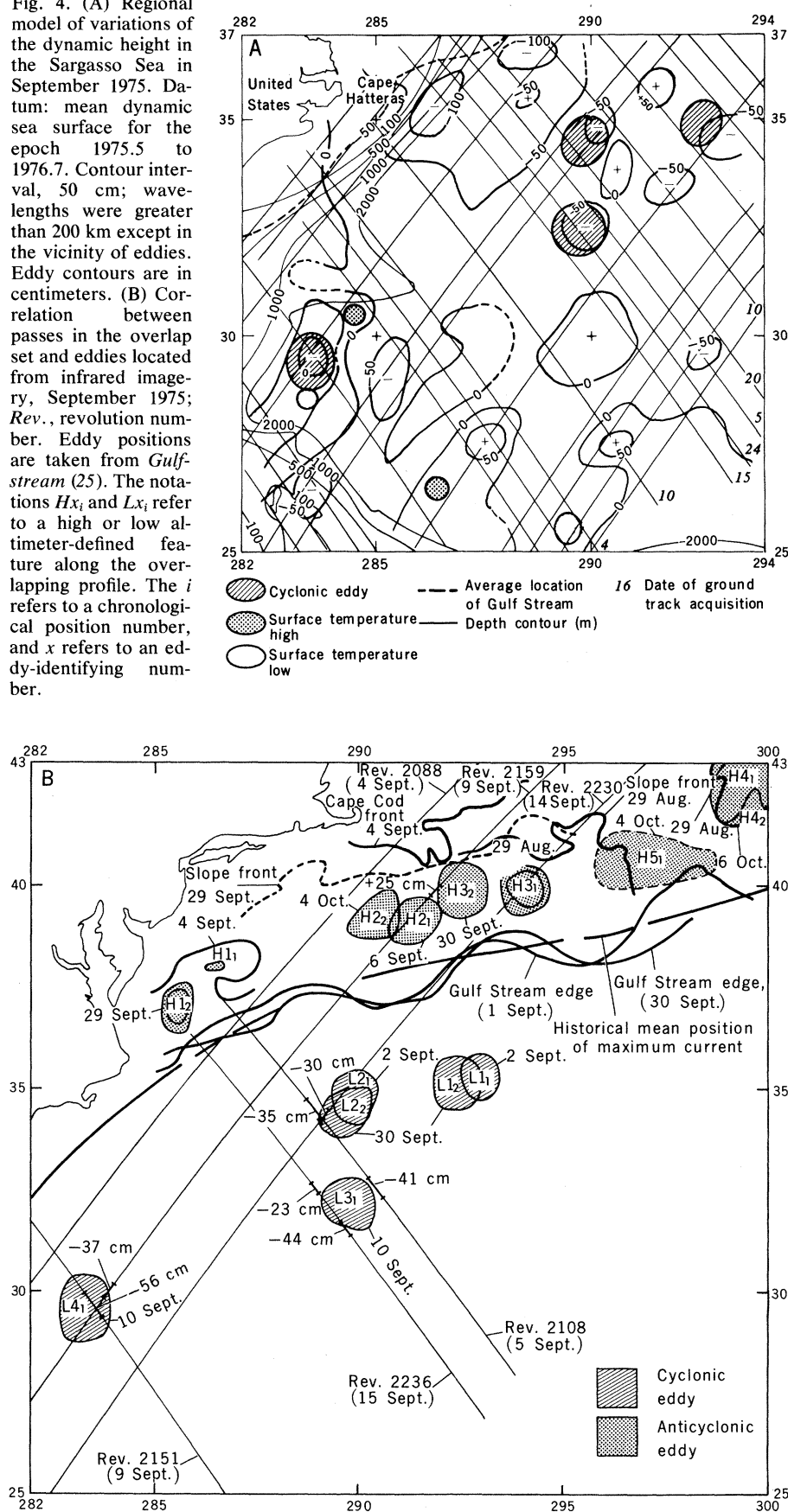
This principle can be used to define regional models of the sea surface in limited areas for the study of time variations in ζ_s and hence the motion of eddies. The area most densely surveyed during the GEOS-3 mission is in the vicinity of the Gulf Stream and the Sargasso Sea to the east of the Gulf Stream in the western North Atlantic (Fig. 4A). Over 250 altimetry passes were acquired in the area. These data were processed to obtain monthly solutions for the shape of the Sargasso Sea from July 1975 to November 1975 and from April 1976 to July 1976 (22). The solution for September 1975 is illustrated in Fig. 4A. The average variability of nontidal heights of the ocean surface models between July 1975 and August 1976 was ± 43 cm (23). Geometrical instability contributes to this figure as the configuration of passes varies from month to month. It drops to ± 33 cm if the peripheries of the region are excluded. Such models appear adequate for the study of variations in ζ_s associated with eddies with amplitudes larger than 50 cm. The ocean tides were treated as a source of random error in these preliminary determinations. In view of the large distance between amphidromes, the major tidal effect is removed in the corrections for b and c . The model shown in Fig. 4A is referred to the mean

sea-surface height for the epoch of measurement at each point and does not contain information on the quasi-stationary components of ζ_s which maintain the

steady-state current systems such as the Gulf Stream.

The variation of ζ_s with time can also be studied along selected profiles of

Fig. 4. (A) Regional model of variations of the dynamic height in the Sargasso Sea in September 1975. Datum: mean dynamic sea surface for the epoch 1975.5 to 1976.7. Contour interval, 50 cm; wavelengths were greater than 200 km except in the vicinity of eddies. Eddy contours are in centimeters. (B) Correlation between passes in the overlap set and eddies located from infrared imagery, September 1975; Rev., revolution number. Eddy positions are taken from *Gulfstream* (25). The notations Hx_i and Lx_i refer to a high or low altimeter-defined feature along the overlapping profile. The i refers to a chronological position number, and x refers to an eddy-identifying number.



overlapping passes; 32 profile sets, having between five and nine overlapping passes in each set, are available in the western North Atlantic (24). Each of these passes is fitted by the application of corrections for b and c to the average of the whole set. Thus, the datum for each set of overlapping passes can be slightly different. The application of b and c corrections removes all information on sea-surface variability with wavelengths in excess of twice the pass length and with periods shorter than that of a single overlap (37.2 days). The average rms discrepancy was ± 33 cm, which is an improvement on the resolution obtained from the set of regional solutions presented here. The disadvantage is the lack of a unique datum for the region and the restricted coverage obtained in both space and time.

The power spectrum of the 32 sets of overlapping passes were analyzed for an estimate of the variability of the oceans in the test area with periods greater than a month and wavelengths between 150 and 5000 km. The value obtained from data recorded between April 1975 and August 1976 was ± 28 cm. Considering the magnitude of unmodeled orbital error, this value is in reasonable agreement with oceanographic estimates and is compatible with the eddy kinetic energy of a wind-driven circulation. Figure 4B shows the layout of passes in the overlap data set for September 1975. A high-pass

filter was used to remove all variations of ζ with wavelengths greater than 100 km. The resulting window was used in the study of eddies.

The location of eddies shown in Fig. 4, A and B, are reported by the National Weather Service from infrared imagery distributed by the National Environmental Satellite Service (25). Both the monthly regional solutions and the overlapping pass sets were examined for correlations with the eddy structures reported. Sea-surface minima occurred within 50 km of the infrared-sensed cyclonic eddies 64 percent of the time and within 100 km on all occasions where altimetry data were available for comparison. In the case of comparisons between ζ maxima and minima from overlapping pass sets, correlations with eddy structures were obtained 58 percent of the time if the criterion was that the altimeter-defined ζ maxima and minima lay within the infrared-defined eddy feature. This correlation increased to 98 percent if instances of partial overlap were also included. The sample sizes were 33 in the case of the regional solution comparisons and 37 for the overlapping pass sets.

In the case of regional solutions, comparisons were also made between highs and lows in ζ and monthly highs and lows in the mean sea-surface temperature. Unfavorable correlations were obtained 16 percent of the time from a sample of 44 comparisons over 10 months. The

slightly inferior level of correlations in this case is not unexpected as surface temperature features do not necessarily correlate with eddies (19).

The Sea Surface Topography Maintaining the Gulf Stream

Regional solutions do not contain information on the quasi-stationary components of ζ_s . Global solutions define ζ_s through those harmonics for which the signal-to-noise ratio is favorable. Neither of these techniques is adequate at the present time for studying variations of ζ_s with position which maintain a dominant steady-state current such as the Gulf Stream. The regional monthly models are consistently biased in relation to the best available geoidal model (26). The contour pattern of the discrepancy D between the sea-surface models from altimetry (after orientation to GEM 9) and the best available gravimetric geoid in the region is regular east of the 2000-m depth contour (Fig. 5A). These contours reflect the errors in the gravimetric geoid and in the quasi-stationary SST if the orientation of the regional models is assumed to be free from error. One cannot separate ζ_s from the sources of error without adopting a speculative assumption about one of the contributory sources to D . The gravimetric geoid is computed at each point from a fixed distribution of

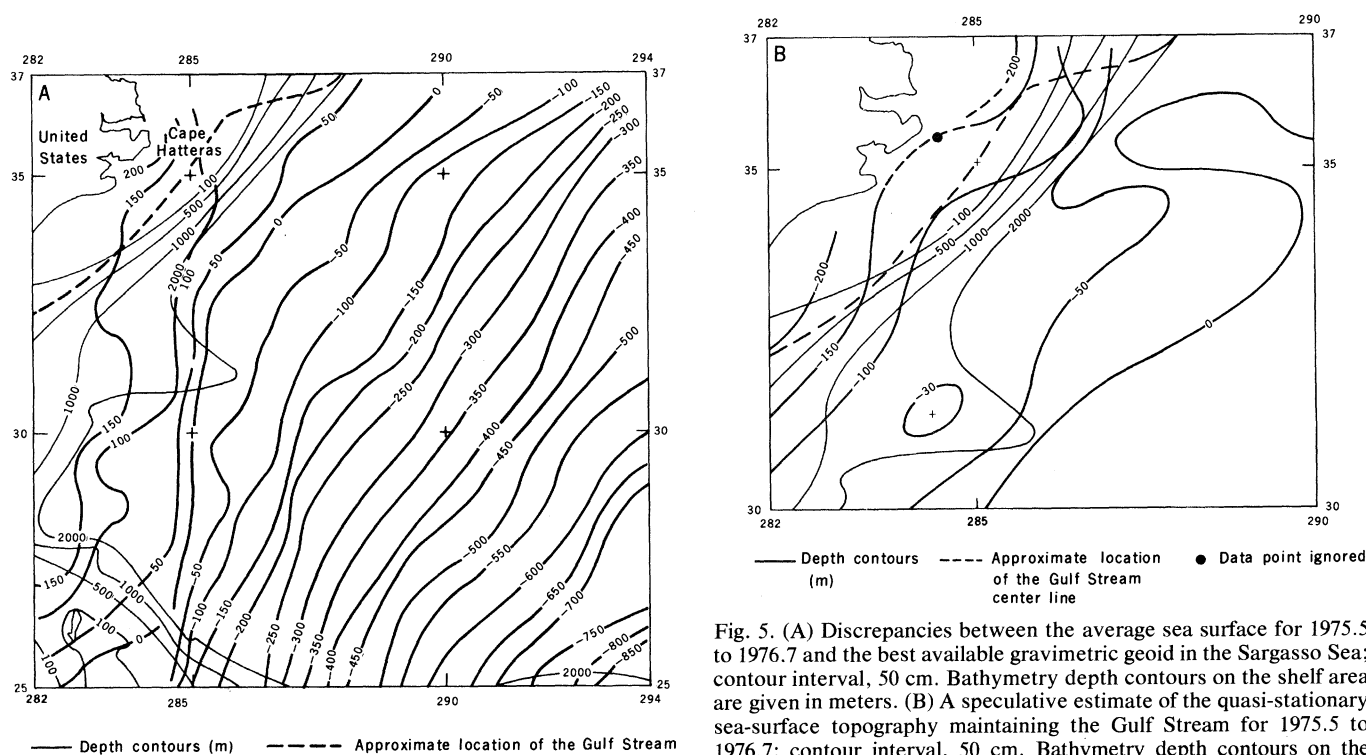


Fig. 5. (A) Discrepancies between the average sea surface for 1975.5 to 1976.7 and the best available gravimetric geoid in the Sargasso Sea; contour interval, 50 cm. Bathymetry depth contours on the shelf area are given in meters. (B) A speculative estimate of the quasi-stationary sea-surface topography maintaining the Gulf Stream for 1975.5 to 1976.7; contour interval, 50 cm. Bathymetry depth contours on the shelf area are given in meters.

data by the use of quadrature techniques (27). The resulting pattern of errors can be expected to vary slowly with position. Linear regression techniques establish the variation (dE/ds) in the geoidal error E along profiles orthogonal to the average direction of the contours east of the 2000-m depth contour, s being the distance from the southeast corner of each profile. The correlation obtained is always better than .99. If it were assumed that this pattern of errors were to continue west of the 2000-m depth contour, the values of ζ_s maintaining the Gulf Stream can be estimated along each profile by means of the relation

$$\zeta_s = D - \frac{dE}{ds} s \quad (6)$$

The resulting contours of ζ_s in the region adjacent to the continental shelf slopes are shown in Fig. 5B. These contours underestimate the quasi-stationary Gulf Stream velocity as being 50 cm/sec, although in the correct direction. These results are presented to illustrate the difficulty of obtaining a reliable estimate of quasi-stationary dynamic SST associated with limited features of the ocean surface circulation from presently available data. The shortcomings are not in the altimetry data themselves but in the best available gravity field and geoid models through the relevant wavelengths.

Conclusions

The analyses described above demonstrate the potential of the satellite altimeter as a tool with which to study the dynamics of the surface layer of the oceans. Sophisticated tracking support is not needed to track eddies, provided 30 passes of data are available each month per 10^6 km^2 in the region of interest. A resolution of $\pm 25 \text{ cm}$ can be expected in such a case. It should also be possible to recover variations with wavelengths between 150 and 5000 km and amplitudes in excess of 30 cm, provided a reliable ocean tide model is available. It is not possible to recover the quasi-stationary component of the SST in this range of

wavelengths unless one makes speculative assumptions.

Acceptable values of the three zonal harmonics of degrees 2, 3, and 4 of the quasi-stationary SST are obtained from global solutions. These contain 75 percent of the strength of signal. Significant gravity field model improvements with a precision of three parts in 10^9 are needed before further advances are possible in this area. No evidence currently exists for any significant widespread discrepancies between satellite and surface oceanographic determinations of the quasi-stationary dynamic SST.

Data collected during the Seasat mission will provide an improved basis for the recovery of ocean dynamic information from radar altimetry for several reasons: (i) a more complete data coverage will be available in both space and time, (ii) the complement of precise tracking systems available is likely to have a better distribution than that used for the GEOS-3 mission, and (iii) the improved gravity fields obtained from the analysis of GEOS-3 data should also provide more precise orbits.

Much work remains to be done on the recovery of oceanographic information from satellite altimetry under adverse signal-to-noise conditions. The oceanographically determined global fields of ζ_s will, in the short term, be useful yardsticks for such studies. Because they can be used to synoptically monitor rapidly changing phenomena, satellite techniques will revolutionize methods in physical oceanography.

References and Notes

1. GEOS-C Mission: Proposal Briefing Information, 13 Dec. 1972 (NASA Wallops Flight Center, Wallops Island, Va., 1972).
 2. The GEOS-3 altimeter also provides data on wave heights by means of a waveform sampling system with 16 sampling gates. These data are not considered in the present article.
 3. R. S. Mather, *UNISURV G* (Aust. J. Geodesy Photogram. Surv.) **24**, 102 (June 1976). Equation 2 relates components of the acceleration (\ddot{x}_1, \ddot{x}_2), velocity (\dot{x}_1, \dot{x}_2), and frictional acceleration (F_1, F_2), due to wind stress acting on the surface layer of the oceans, to the horizontal gradients of the sea-surface topography (ζ_s) and atmospheric pressure (p_a). In Eq. 2, g is the value of gravity and ρ_w is the density of seawater. The quantity x_1, x_2 is a local two-dimensional Cartesian coordinate system with the x_1 axis oriented east and the x_2 axis oriented north in the local horizon. If ϕ is the latitude and λ is the longitude, f is the Coriolis parameter related to the rotation rate ω of the earth given by the relation $f = 2\omega \sin\phi$. The effect of wind on the surface layer dynamics can be empirically approximated by
- $$F_i = \frac{K[w_1^2 + w_2^2]^{1/2}}{\rho_w H} w_i$$
- where K is an empirically derived drag coefficient ($2 \times 10^{-6} < K < 2.6 \times 10^{-6}$), H is the thickness of the mixed (Ekman) layer (in centimeters), and w_i represents the wind speed components (in centimeters per second).
4. G. Neumann, *Ocean Currents* (Elsevier, Amsterdam, 1966).
 5. R. S. Mather, F. J. Lerch, C. Rizos, E. G. Masters, B. Hirsch, *NASA Tech. Mem.* 79558 (May 1978).
 6. The laser orbits were prepared under the supervision of F. J. Lerch of GSFC at Wolf Corporation by S. M. Klosko.
 7. F. J. Lerch, S. M. Klosko, R. E. Laubscher, C. A. Wagner, *Gravity Field Model Improvement Using GEOS-3 (GEM 9 and 10)* (NASA-GSFC Document X-921-77-246, Goddard Space Flight Center, Greenbelt, Md., 1977).
 8. Examples of techniques for such determination are given in W. A. Heiskanen and H. Moritz, *Physical Geodesy* (Freeman, San Francisco, 1967).
 9. The normalized associated Legendre function $P_{nm}(\mu)$ is given by
- $$P_{nm}(\mu) = \left[\frac{(2 - \delta_{0m})(2n+1)(n-m)!}{(n+m)!} \right]^{1/2} \frac{(1 - \mu^2)^{m/2}}{2^n} \times \sum_{r=0}^k (-1)^r \frac{(2n-2r)!}{r!(n-m-2r)!(n-r)!} \mu^{n-m-2r}$$
- where k is the truncated integer $(n-m)/2$; δ_{0m} is the Kronecker delta; $\mu = \sin \phi$, where ϕ is latitude; and r is an index of summation, which takes values of 0 to k .
10. D. Y. Lai and P. L. Richardson, *J. Phys. Oceanogr.* **7** (No. 5), 670 (1977).
 11. For a description of the oceanographic model, see (5), p. 3.
 12. R. S. Mather, *NASA Tech. Mem.* 79540 (May 1978), pp. 12-13.
 13. For the extent of variations, see (5), p. 15.
 14. For more details, see (5), p. 6.
 15. Annual reports on the maintenance of this system are issued by the Bureau International de l'Heure, Paris.
 16. R. S. Mather, *UNISURV G* (Aust. J. Geodesy Photogram. Surv.) **28**, 76 (June 1978).
 17. K. Wyrski, L. Magaard, K. Hager, *J. Geophys. Res.* **81**, 2645 (1976).
 18. P. M. Saunders, *Deep-Sea Res.* **18**, 1215 (1971).
 19. R. E. Cheney and P. L. Richardson, *ibid.* **23**, 145 (1976).
 20. The Nyquist frequency, $f_N = 1/(2\Delta)$, is the highest frequency that can be detected with data sampled at intervals Δ .
 21. An initial study of overlapping passes is reported by R. S. Mather, R. Coleman, C. Rizos, B. Hirsch, *UNISURV G* (Aust. J. Geodesy Photogram. Surv.) **26**, 27 (June 1977).
 22. Details are reported in R. S. Mather, R. Coleman, B. Hirsch, *NASA Tech. Mem.* 79549 (May 1978).
 23. For the distribution of the variability as a function of position, see (22), p. 45.
 24. For further details, see (22), pp. 2 and 8.
 25. A monthly summary of data is given in the publication *Gulfstream* (U.S. National Weather Service, National Oceanic and Atmospheric Administration, Washington, D.C.).
 26. For further discussion, see (22), pp. 13-14.
 27. The best available gravimetric geoid for the area is illustrated in J. G. Marsh and E. S. Chang, *Mar. Geodesy* **1** (No. 3), 1 (1978), figure 1.